Journal of Thermal Stresses
Publication details, including instructions for authors and subscription information:
http://www.tandfonline.com/loi/uths20

A Theoretical Analysis on the Thermal Buckling Behavior of Fully Clamped Sandwich Panels with Truss Cores

Wu Yuan [a], Xi Wang [a], Hongwei Song [a] & Chenguang Huang [a]
[a] Key Laboratory for Mechanics in Fluid Solid Coupling Systems, Institute of Mechanics, Chinese Academy of Sciences, Beijing, China
Published online: 03 Sep 2014.

Journal of Thermal Stresses, 37: 1433–1448, 2014

ISSN: 0149-5739 print/1521-074X online
DOI: 10.1080/01495739.2014.937263

A THEORETICAL ANALYSIS ON THE THERMAL BUCKLING BEHAVIOR OF FULLY CLAMPED SANDWICH PANELS WITH TRUSS CORES

Wu Yuan, Xi Wang, Hongwei Song, and Chenguang Huang
Key Laboratory for Mechanics in Fluid Solid Coupling Systems, Institute of Mechanics, Chinese Academy of Sciences, Beijing, China

This article presents a theoretical analysis on the thermal buckling behavior of sandwich panels with truss cores under fully clamped boundary conditions, subjected to uniform temperature rise. The Reissner model is developed by ignoring the flexural rigidity of the core and considering the shear stiffness of the sandwich panel is only contributed by truss cores. By using double Fourier expansions to the virtual deformation mode, the critical temperature of sandwich panels is obtained. Theoretically predicted critical temperatures are in good agreement with those from FEM. The effect of boundary conditions and structure parameters of the sandwich panel are also discussed.

Keywords: Reissner model; Sandwich panel; Thermal buckling; Truss cores

1. INTRODUCTION

Due to the lightweight and multifunctional characteristics, cellular materials and their sandwich structures have been extensively investigated for their fundamental properties [1–7] and applications in thermal insulation, heat transfer enhancement, shock resistance, energy absorption, etc. [8–14]. Among them, sandwich panels with truss cores have been proposed recently and have demonstrated significant advantages [3, 7, 15–19]. They have been considered as promising candidates for the lightweight design and thermal protection structures utilized in high-speed flight. When being used as load-bearing components in a thermal protection system, the sandwich panel experiences large temperature changes and may buckle due to the in-plane load caused by the constrained thermal expansion. Likewise, thermal buckling is one of the most pressing issues in the advancement of high-speed flight. For example, during X-15 flights, windshield damage occurred when thermal buckling of the retainer frame caused intense local heating in the glass [20]. Therefore, it is imperative to carry out theoretical studies on the thermal buckling behavior of sandwich panels with truss cores.

Received 21 February 2014; accepted 1 April 2014.
Address correspondence to Hongwei Song, Key Laboratory for Mechanics in Fluid Solid Coupling Systems, Institute of Mechanics, Chinese Academy of Sciences, No.15 Beisihuanxi Road, Beijing 100190, China. E-mail: songhw@imech.ac.cn
Color versions of one or more of the figures in the article can be found online at www.tandfonline.com/uths.

Previous theoretical researches mainly focus on the buckling and post-buckling behavior of thin plates and thin laminates. Mossavarali and Eslami [21] studied the post-buckling of a thin plate, which has initial flaws. Fu [22] studied the buckling behavior of plates at various complex boundary conditions by using the reciprocal theorem. Raju et al. [23] analyzed the thermal buckling behavior of circular plates with localized axisymmetric damages. The effect of transverse shear deformation across the thickness was ignored by the preceding studies. For a sandwich panel with truss cores, which has poor shear stiffness, ignorance of the transverse shear effect may result in a big error.

So far, there have been a number of theoretical models developed on sandwich panels, such as the Reissner model [24], Hoff model [25], and Tu model [26], etc. The overwhelming majority of the available analytical solutions reported in the literature have been obtained for sandwich plates with simply supported edges (SSSS plates) [27]. Chen et al. [28] analyzed the buckling behavior of SSSS sandwich panels with metallic truss cores using Reissner's model.

For sandwich panels under fully clamped conditions (CCCC), the critical buckling temperature cannot be analytically solved as one under simply supported conditions, since governing equations for the deformation mode are complicated due to complex boundary conditions. Lopatina and Morozovb [27] proposed a solution to the buckling problem formulated for a rectangular sandwich plate having all the edges fully clamped (CCCC plate) and subjected to a uniaxial compressive loading. Al-Khaleefi and Kabir [29] considered plates with fully clamped boundary conditions where displacement solution functions were assumed in the form of two sets of double Fourier series expansions. For sandwich panels with truss cores, which have weak cores and thin sheets, the thermal buckling behavior has not been systematically investigated.

Within the authors' knowledge, there have been few theoretical studies reported on the thermal buckling of sandwich panels with truss cores, especially under CCCC conditions. This article adopts first-order deformation theory and assumes the truss core is a continuous material. Using Reissner's model, the critical buckling temperature of CCCC sandwich panels subjected to uniform temperature rise is solved through the method of double Fourier expansions to the virtual deformation mode. Theoretically predicted critical buckling temperatures agree well with those obtained from numerical models.

THEORETICAL ANALYSIS

Here, a Reissner model is developed to analyze the thermal buckling behavior of the CCCC sandwich panel with truss cores. Sandwich panels with truss cores of importance are illustrated in Figure 1. According to the geometry of the unit truss cell, sandwich panels can be classified in pyramidal, tetrahedral, and Kagome configurations. The fundamental mechanical property of various truss cores have been investigated extensively, and elastic constants can be conveniently obtained. For example, Deshpande et al. [2] gave the three-dimensional elastic constitutive relation of lattice truss cores. In the present work, the face sheet and core of sandwich panels are made of identical metal materials that can resist high temperature, and the face sheet is very thin. Figure 2 shows the schematic of the

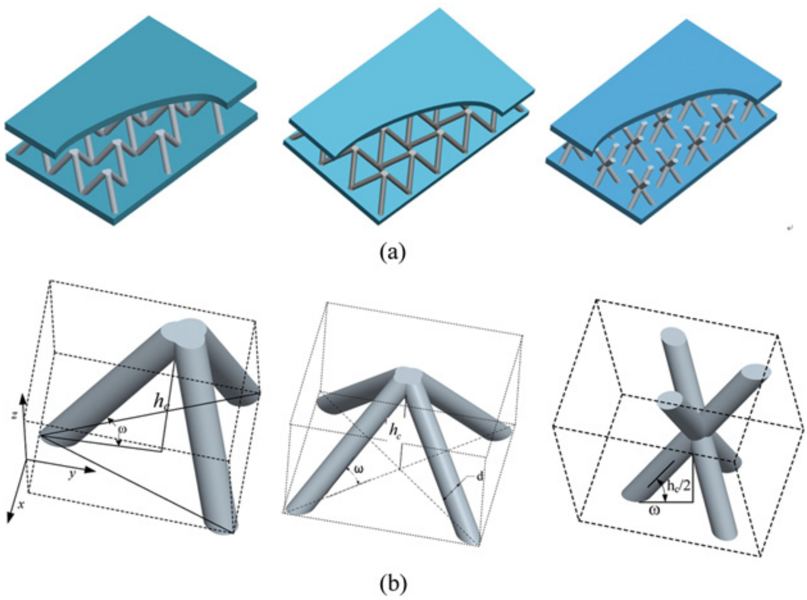

Figure 1 Schematics of sandwich panels with truss cores: (a) Sandwich panels with truss cores: tetrahedral, pyramidal, and Kagome configuration; (b) representative cell of truss cores: tetrahedral, pyramidal, and Kagome.

equivalent analytical model. The sandwich panel is in the dimension of length a, width b, and total thickness h_p, and the thickness of the core is h_c. Because the shear stiffness of the core is relatively low, and the flexural rigidity of the face sheet is high, the following assumptions are made:

1. The size of the unit truss cell is small, compared to the size of the sandwich panel, therefore truss cores are considered as continuous and homogeneous.
2. The truss core is pin-jointed and does not contribute to the overall flexural rigidity.
3. The transverse shear stiffness of the sandwich panel is only contributed by the truss core.
4. The deformation of the sandwich panel is very small, and straight lines normal to the middle plane remain straight in distortion, but rotate through a small angle due to transverse deformation.

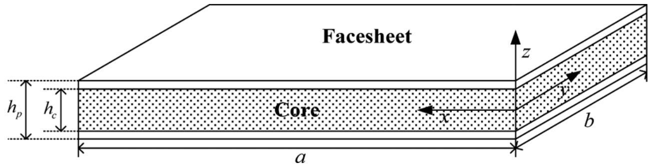

Figure 2 Equivalent analytical model.

The displacement field of the sandwich panel based on the first-order theory can be expressed as

$$
\begin{aligned}
u(x, y) &= -z\phi_x(x, y) \\
v(x, y) &= -z\phi_y(x, y) \\
w(x, y) &= w_0(x, y)
\end{aligned}
\tag{1}
$$

where u, v and w are displacements in x, y, and z directions, while ϕ_x and ϕ_y are rotations of the normal in the xz and yz planes, respectively. Additionally, w_0 is the displacement of the middle plane.

According to Hooke's law, stresses in the sandwich panel are expressed as

$$
\begin{aligned}
\sigma_x &= \frac{E}{1-\mu^2}\left(\frac{\partial u}{\partial x} + \mu\frac{\partial v}{\partial y}\right) \\
\sigma_y &= \frac{E}{1-\mu^2}\left(\mu\frac{\partial u}{\partial x} + \frac{\partial v}{\partial y}\right) \\
\tau_{xy} &= \frac{E}{2(1+\mu)}\left(\frac{\partial u}{\partial y} + \frac{\partial v}{\partial x}\right)
\end{aligned}
\tag{2}
$$

where E and μ are the elastic modulus and Poisson ratio of the panel material, respectively.

According to assumptions made earlier, equations of internal force can be derived

$$
\begin{aligned}
M_x &= -D\left(\frac{\partial \phi_x}{\partial x} + \mu\frac{\partial \phi_y}{\partial y}\right) \\
M_y &= -D\left(\frac{\partial \phi_y}{\partial y} + \mu\frac{\partial \phi_x}{\partial x}\right) \\
M_{xy} &= -\frac{D}{2}(1-\mu)\left(\frac{\partial \phi_x}{\partial y} + \frac{\partial \phi_y}{\partial x}\right) \\
Q_x &= C\left(\frac{\partial w}{\partial x} - \phi_x\right) \\
Q_y &= C\left(\frac{\partial w}{\partial y} - \phi_y\right) \\
C &= G_c h_c \\
D &= \frac{E(h_p^3 - h_c^3)}{12(1-\mu^2)}
\end{aligned}
\tag{3}
$$

where C and D are the shear stiffness and flexural rigidity of the sandwich panel, respectively, and G_c is the equivalent shear modulus of the lattice truss core.

Equilibrium equations of the plate can be expressed as

$$
\frac{\partial M_x}{\partial x} + \frac{\partial M_{xy}}{\partial y} - Q_x = 0
$$

$$\frac{\partial M_{xy}}{\partial x} + \frac{\partial M_y}{\partial y} - Q_y = 0 \tag{4}$$

$$\frac{\partial Q_x}{\partial x} + \frac{\partial Q_y}{\partial y} + N_x \frac{\partial^2 w}{\partial x^2} + 2N_{xy} \frac{\partial^2 w}{\partial x \partial y} + N_y \frac{\partial^2 w}{\partial y^2} = 0$$

When applying a thermal load due to a uniform temperature rise, the bi-axial compressive in-plane force can be expressed as

$$\begin{aligned} N_x &= N_y = -\frac{E\alpha}{1-\mu}(h_{\mathrm{p}} - h_{\mathrm{c}})\Delta T = N \\ N_{xy} &= 0 \end{aligned} \tag{5}$$

where α and $\Delta T$are coefficient of thermal expansion and the temperature rise of the sandwich panel, respectively.

Substituting Eq. (3) and Eq. (5) into Eq. (4), equilibrium equations of the sandwich panel with truss cores can be obtained

$$\begin{aligned} &D\left(\frac{\partial^2 \phi_x}{\partial x^2} + \frac{1-\mu}{2}\frac{\partial^2 \phi_x}{\partial y^2} + \frac{1+\mu}{2}\frac{\partial^2 \phi_y}{\partial x \partial y}\right) + C\left(\frac{\partial w}{\partial x} - \phi_x\right) = 0 \\ &D\left(\frac{\partial^2 \phi_y}{\partial y^2} + \frac{1-\mu}{2}\frac{\partial^2 \phi_y}{\partial x^2} + \frac{1+\mu}{2}\frac{\partial^2 \phi_x}{\partial x \partial y}\right) + C\left(\frac{\partial w}{\partial y} - \phi_y\right) = 0 \\ &D\left(\frac{\partial^2 w}{\partial x^2} + \frac{\partial^2 w}{\partial y^2} - \frac{\partial \phi_x}{\partial x} - \frac{\partial \phi_y}{\partial y}\right) + N\nabla^2 w = 0 \end{aligned} \tag{6}$$

Consider the CCCC boundary condition,

$$\begin{aligned} x &= 0, \quad a : w = \phi_x = \phi_y = 0 \\ y &= 0, \quad b : w = \phi_x = \phi_y = 0 \end{aligned} \tag{7}$$

The following virtual displacement mode is assumed [30]:

$$\begin{aligned} w &= \sum_{m=1}^{\infty}\sum_{n=1}^{\infty} A_{mn} \sin \alpha_m x \, \sin \beta_n y \\ \phi_x &= \sum_{m=1}^{\infty}\sum_{n=1}^{\infty} B_{mn} \sin \alpha_m x \sin \beta_n y \\ \phi_y &= \sum_{m=1}^{\infty}\sum_{n=1}^{\infty} C_{mn} \sin \alpha_m x \sin \beta_n y \end{aligned} \tag{8}$$

where A_{mn}, B_{mn} and C_{mn} are Fourier constant coefficients, and α_m and β_n are defined as $\frac{m\pi}{a}$ and $\frac{n\pi}{b}$, respectively.

Substituting Eq. (8) into Eq. (6) yields the following sets of equations:

$$\sum_{m=1}^{\infty}\sum_{n=1}^{\infty}\left(\frac{\mu-1}{2} DB_{mn}\beta_n^2 - DB_{mn}\alpha_m^2 - CB_{mn}\right)\sin(\alpha_m x)\sin(\beta_n y)$$

$$
\begin{aligned}
&+\sum_{m=1}^{\infty}\sum_{n=1}^{\infty} CA_{mn}\alpha_m \cos(\alpha_m x)\sin(\beta_n y)\\
&+\sum_{m=1}^{\infty}\sum_{n=1}^{\infty} \frac{1+\mu}{2} DC_{mn}\alpha_m\beta_n \cos(\alpha_m x)\cos(\beta_n y) = 0\\
&\sum_{m=1}^{\infty}\sum_{n=1}^{\infty}\left(\frac{\mu-1}{2}DC_{mn}\alpha_m^2 - DC_{mn}\beta_n^2 - CC_{mn}\right)\sin(\alpha_m x)\sin(\beta_n y)\\
&+\sum_{m=1}^{\infty}\sum_{n=1}^{\infty} CA_{mn}\beta_n \sin(\alpha_m x)\cos(\beta_n y)\\
&+\sum_{m=1}^{\infty}\sum_{n=1}^{\infty} \frac{1+\mu}{2} DB_{mn}\alpha_m\beta_n \cos(\alpha_m x)\cos(\beta_n y) = 0\\
&\sum_{m=1}^{\infty}\sum_{n=1}^{\infty}[-(C+N)(A_{mn}\alpha_m^2 + A_{mn}\beta_n^2)]\sin(\alpha_m x)\sin(\beta_n y)\\
&-\sum_{m=1}^{\infty}\sum_{n=1}^{\infty} CC_{mn}\beta_n \sin(\alpha_m x)\cos(\beta_n y)\\
&-\sum_{m=1}^{\infty}\sum_{n=1}^{\infty} CB_{mn}\alpha_m \cos(\alpha_m x)\sin(\beta_n y) = 0
\end{aligned} \tag{9}
$$

To solve Eq. (9), $\cos(\alpha_m x)$, $\cos(\beta_n y)$ and $\cos(\alpha_m x)\cos(\beta_n y)$ are expanded into the following forms:

$$
\begin{aligned}
\cos(\alpha_m x)\cos(\beta_n y) &= \sum_{r=1}^{\infty}\sum_{s=1}^{\infty} h_{rm}h_{sn}\sin(\gamma_r x)\sin(\psi_s y)\\
&\quad 0 < x < a,\ 0 < y < b\\
\cos(\alpha_m x) &= \sum_{r=1}^{\infty} h_{rm}\sin(\gamma_r x)\\
&\quad 0 < x < a\\
\cos(\beta_n y) &= \sum_{s=1}^{\infty} h_{sn}\sin(\psi_s y)\\
&\quad 0 < y < b
\end{aligned} \tag{10}
$$

where

$$
\begin{aligned}
h_{rm} &= \frac{4m}{\pi(m^2 - r^2)}\\
h_{sn} &= \frac{4n}{\pi(n^2 - s^2)}
\end{aligned} \tag{11}
$$

and

$$
\gamma_r = \frac{r\pi}{a}, \quad \psi_s = \frac{s\pi}{b}
$$

Introducing Eq. (10) and Eq. (11) into Eq. (9), one yields

$$\begin{aligned}
&\sum_{m=1}^{\infty}\sum_{n=1}^{\infty}\left(\frac{\mu-1}{2}D\beta_n^2 - D\alpha_m^2 - C\right)B_{mn} + \sum_{r=1}^{\infty} h_{rm}CA_{rn}\gamma_r \\
&\quad + \sum_{r=1}^{\infty}\sum_{s=1}^{\infty} h_{rm}h_{sn}\frac{1+\mu}{2}DC_{rs}\gamma_r\psi_s = 0 \\
&\sum_{m=1}^{\infty}\sum_{n=1}^{\infty}\Bigg\{(\frac{\mu-1}{2}D\alpha_m^2 - D\beta_n^2 - C)C_{mn} + \sum_{s=1}^{\infty} h_{sn}CA_{ms}\psi_s \\
&\quad + \sum_{r=1}^{\infty}\sum_{s=1}^{\infty} h_{rm}h_{sn}\frac{1+\mu}{2}DB_{rs}\gamma_r\psi_s\Bigg\} = 0 \\
&\sum_{m=1}^{\infty}\sum_{n=1}^{\infty}\Bigg\{-[C(A_{mn}\alpha_m^2 + A_{mn}\beta_n^2)] \\
&\quad - \sum_{s=1}^{\infty} h_{sn}CC_{ms}\psi_s - \sum_{r=1}^{\infty} h_{rm}CB_{rn}\gamma_r\Bigg\} - N\sum_{m=1}^{\infty}\sum_{n=1}^{\infty}[(A_{mn}\alpha_m^2 + A_{mn}\beta_n^2)] = 0 \qquad (12)
\end{aligned}$$

SOLUTIONS

To solve Eq. (12), we cast it in a form of eigenvalue solution that can be written as

$$\left[\underset{\sim}{K} + \lambda \underset{\sim}{K}_G\right]\left[\underset{\sim}{u}\right] = 0 \qquad (13)$$

where $\underset{\sim}{K}$ contains coefficients related to geometry generated from Eq. (12), and $\underset{\sim}{K}_G$ contains coefficients related to thermal effects. $[\underset{\sim}{u}]$ contains unknown constant Fourier coefficients, λ represents the critical buckling temperature. A computer program called "Thermal buckling" in FORTRAN code was developed to solve Eq. (13) by calling the subroutine GVCRG of IMSL, which is used to solve eigenvalue problems. Table 1 gives geometric parameters and material properties used to calculate the critical buckling temperature according to the present theory. The material properties are based on stainless steel, which has a maximum usage temperature of 750°. To study the convergence of double Fourier expansions, the critical buckling temperature is computed with $m = n$. Figure 3 shows the variation of calculated critical buckling temperatures as m and n increases. A reasonable convergence is reached after $m = n \geq 10$.

Table 1 Parameters used to obtain the theoretical prediction of the critical buckling temperature

h_c (mm)	h_p (mm)	E (GPa)	μ	α ($\times 10^{-6}$)	a (mm)	b (mm)
8	10	200	0.3	16	300	300

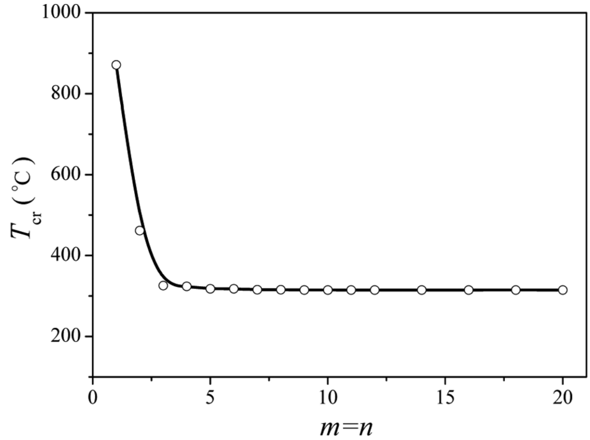

Figure 3 Convergence of critical buckling temperature with m and n.

NUMERICAL MODELING

To verify the accuracy of the theoretical prediction, a 3D full-size finite element model was also established to solve the critical buckling temperature by using the commercial code ABAQUS. The sandwich panel is loaded in a uniform temperature field, and the critical buckling temperature can be obtained through solving the eigenvalue of the stiffness matrix of the sandwich panel. Due to the symmetrical characteristics of the sandwich panel and boundary conditions, a one-quarter model is adopted.

In-plane and out-of-plane motions of two edges of the sandwich panel are constrained to make the fully clamped boundary conditions, and the in-plane motion and rotation are restricted at the other two edges to make the symmetrical boundary conditions. Figure 4 shows the finite element model and the buckling mode. The face sheet and truss cores are modeled with shell and beam element, respectively. The relative density of truss cores can be varied by changing the cross-sectional area of the beam element:

$$\begin{aligned}
\bar{\rho}_{\text{tet}} &= \frac{2\sqrt{3}A\sin\omega}{h_c^2} \\
\bar{\rho}_{\text{pyramid}} &= \frac{4A\sin\omega}{h_c^2} \\
\bar{\rho}_{\text{Kagome}} &= \frac{3A}{h_d^2\sin\omega}
\end{aligned} \tag{14}$$

where A is the cross-sectional area of the beam element, and h_d is the distance between unit truss cell of the Kagome configuration, see Figure 1b.

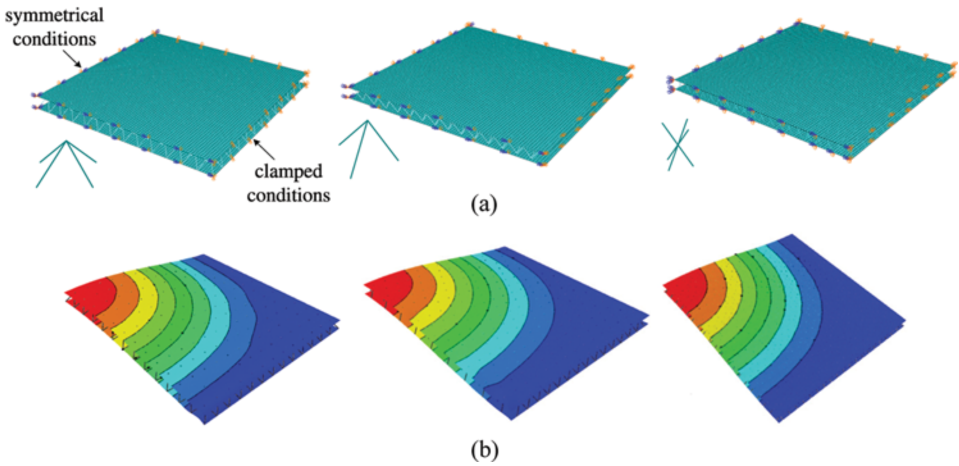

Figure 4 Finite element models and buckling modes of sandwich panels with truss cores, 1/4 model: (a) Finite element models: pyramidal, tetrahedral, and Kagome configurations; (b) buckling modes: pyramidal, tetrahedral, and Kagome configurations.

RESULTS AND DISCUSSIONS

Comparison between Theoretical Prediction and Numerical Analysis

Figure 5 shows the comparison between the theoretical prediction and numerical analysis. The critical buckling temperature of sandwich panels obtained by theoretical prediction is in good agreement with the result from the finite element analysis, which is a reasonable validation for the analytical model.

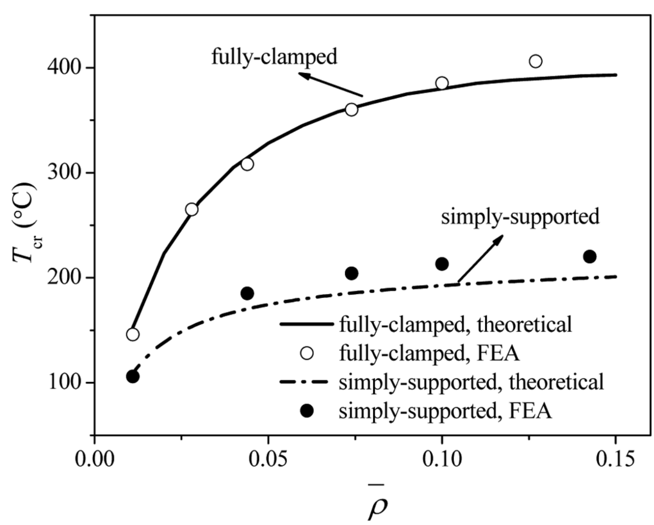

Figure 5 Comparison between theoretical prediction and finite element analysis.

Effects of Boundary Conditions

For the thermal buckling of sandwich panels with truss cores under SSSS conditions, the boundary condition can be written as

$$\begin{aligned} x = 0, a : w = \phi_x = 0 \\ y = 0, b : w = \phi_y = 0 \end{aligned} \tag{15}$$

and the following virtual displacement modes are assumed:

$$\begin{aligned} \phi_x &= u_0 \cos \alpha_k x \sin \beta_l y \\ \phi_y &= v_0 \cos \beta_l y \sin \alpha_k x \\ w &= w_0 \sin \alpha_k x \sin \beta_l y \end{aligned} \tag{16}$$

Substituting Eq. (16) into equilibrium equation Eq. (6), the critical buckling temperature of sandwich panels with truss cores under SSSS conditions can be obtained:

$$T_{\mathrm{cr}} = \frac{(1-\mu)N}{E\alpha(h_{\mathrm{p}} - h_{\mathrm{c}})} \tag{17}$$

where

$$N = \frac{DC\pi^2(a^2l^2 + b^2k^2)}{Ca^2b^2 + D\pi^2(a^2l^2 + b^2k^2)}$$

The comparison of critical buckling temperature between SSSS and CCCC conditions is shown in Figure 5. Under CCCC conditions, not only in-plane and out-of-plane motions but also rotations at edges are restricted. Therefore, the stability of the sandwich panels under CCCC conditions is significantly improved. As a result, critical buckling temperatures under CCCC conditions are much higher than those under SSSS conditions.

Effects of Truss Configuration

For sandwich panels with truss cores subjected to out-of-plane compression, buckling of the elements of the truss is the most common failure mode. In the present thermal buckling analysis, the panel is subjected to in-plane compression, and the in-plane loads are mainly carried by the face sheets whereas the truss elements mainly bear the shearing force. The axial compressive force applied to the truss elements is small and can be neglected. Therefore, the buckling of the elements of the truss is not likely happen in the thermal buckling analysis.

For the three types of sandwich panels illustrated in Figure 1, the shear stiffness can be derived:

$$\begin{aligned} C_{\mathrm{pyramid}} &= G_{\mathrm{pyramid}} h_{\mathrm{c}} = \frac{1}{8}\bar{\rho} E h_{\mathrm{c}} \\ C_{\mathrm{tet}} = C_{\mathrm{kagome}} &= G_{\mathrm{tet}} h_{\mathrm{c}} = \frac{1}{9}\bar{\rho} E h_{\mathrm{c}} \end{aligned} \tag{18}$$

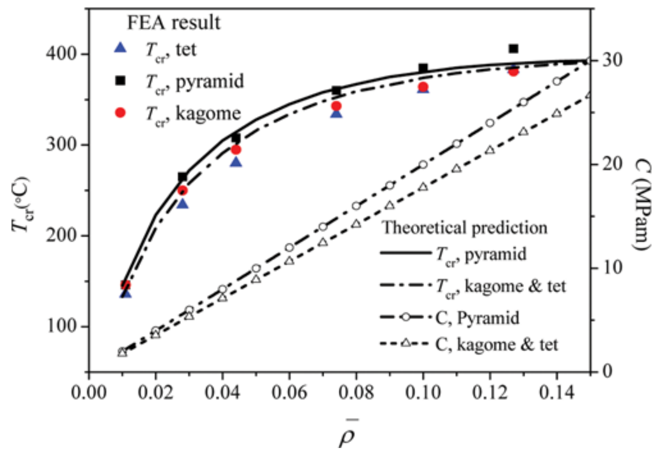

Figure 6 Comparison of critical buckling temperature and shear stiffness of different cell configurations.

Eq. (18) was obtained from relations between the shearing force and the displacement as described in the Appendix. According to Eq. (18), the shear stiffness of the pyramidal truss core is greater than that of the Kagome and tetrahedral core, when they are in the same relative density. The theoretical analysis shows that the stability of sandwich panels is directly related to the shear stiffness. Therefore, critical buckling temperatures of sandwich panels with pyramidal truss cores should be greater than those of the other two configurations. Figure 6 shows that both theoretical predictions and finite element results are both in accordance with this tendency. Critical buckling temperatures of pyramidal configurations are slightly higher than the other two configurations.

Effects of Relative Density and Facesheet Thickness

As shown in Figure 5 and Figure 6, the critical buckling temperature of the sandwich panel increases as the relative density grows, whereas the tendency become stable when the relative density is greater than 0.1. This means, for a sandwich panel, the resistance to thermal buckling can be improved by using higher relative density truss cores, whereas it maybe not as efficient when the relative density is higher than 0.1. As shown in Figure 7, the ratio of critical buckling temperature to the volume of truss core, T_{cr}/V (representation of specific stiffness per unit volume) is introduced to denote the thermal buckling load per unit volume. As the relative density grows, the specific stiffness of the sandwich panel climbs to the top when the relative density is about 0.08, and then drops.

Figure 8 shows the influence of the face sheet thickness. In-plane load increases when the thickness of the face sheet grows, whereas the shear stiffness of the truss core is still weak, and an increase in thickness may result in decrease in the critical buckling temperature.

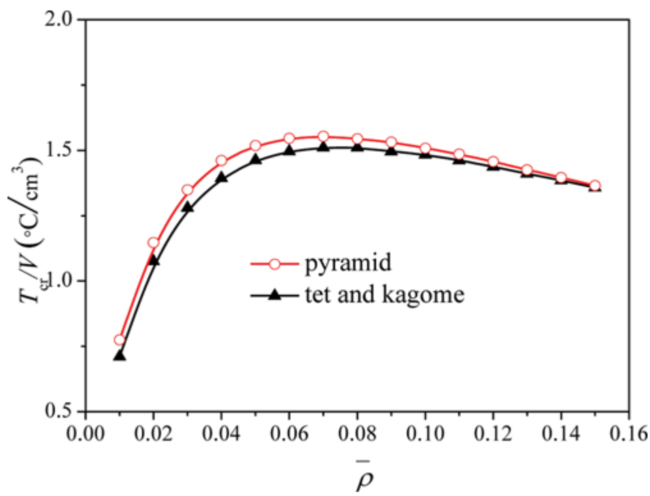

Figure 7 Thermal buckling load per unit volume versus relative density.

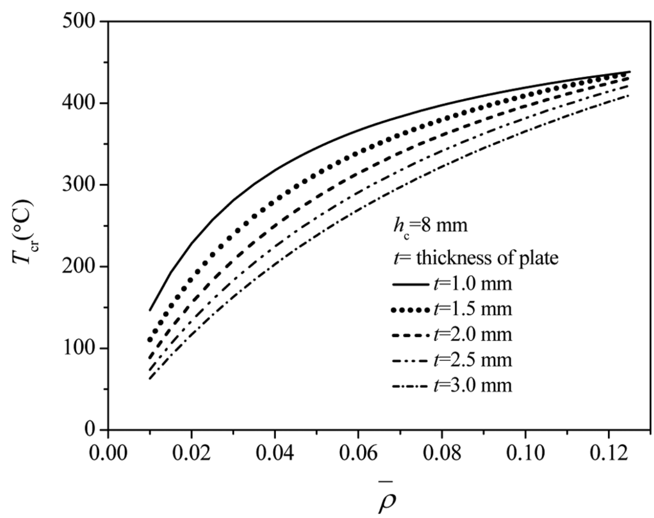

Figure 8 Critical buckling temperature versus relative density of various face sheet thicknesses.

CONCLUSIONS

An analytical model for the thermal buckling of fully clamped sandwich panels with truss cores subjected to a uniform temperature rise was developed by using the Reissner model. Critical buckling temperatures of sandwich panels under CCCC conditions are obtained through numerical iterative approaches. Theoretical results are in good agreement with those of finite element analysis. According to the theoretical analysis, the influence of boundary condition, truss core configuration, relative density and thickness of face sheet to the critical buckling temperature is also discussed.

The stability of the sandwich panel under CCCC conditions is significantly improved, and the critical buckling temperature is much higher, when compared with that under SSSS conditions. The resistance to thermal buckling of the sandwich panel can be improved using higher relative density truss cores. However, when the relative density is greater than 0.08, increase in the relative density demonstrates low efficiency. The shear stiffness of pyramidal truss cores is greater than that of Kagome and tetrahedral cores; therefore, the critical buckling temperature of sandwich panels with pyramidal truss cores is the highest of the three configurations. In addition, increase in plate thickness may result in decrease in critical buckling temperature.

The metallic sandwich panel with truss core may demonstrate multiple failure mechanisms under various loadings. For metallic sandwich panels subject to bending, Rathbun et al. [31] summarized four possible failure modes: face yielding, face buckling, core yielding, and core buckling. There are competitions between different failure mechanisms. In the present study, local face yielding (or facings losing strength), and overall panel buckling are the two most likely failure modes for sandwich panels. This article provides a tool to predict at which temperature level buckling may occur. Whether local face yielding happened before overall panel buckling should be examined through future experimental study.

APPENDIX

The shear stiffness of the sandwich panel is derived by considering the deformation of one unit cell. When applying a shear force Fon one side of the panel, the displacement of the three configurations can be expressed as

$$\begin{aligned} \Delta_{\text{pyramid}} &= \frac{Fh_c}{2EA\sin^3\omega} \\ \Delta_{\text{tet}} &= \frac{4Fh_c}{3EA\sin^3\omega} \\ \Delta_{\text{Kagome}} &= \frac{4\sqrt{3}Fh_c}{6\sqrt{2}EA\cos^2\omega} \end{aligned} \tag{A.1}$$

The shearing strain can be derived:

$$\begin{aligned} \gamma_{\text{pyramid}} &= \frac{\Delta}{h_c} = \frac{F}{2EA\sin^3\omega} \\ \gamma_{\text{tet}} &= \frac{\Delta}{h_c} = \frac{4F}{3EA\sin^3\omega} \\ \gamma_{\text{Kagome}} &= \frac{\Delta}{h_c} = \frac{4\sqrt{3}F}{6\sqrt{2}EA\cos^2\omega} \end{aligned} \tag{A.2}$$

Then the shear modulus can be obtained:

$$G_{\text{pyramid}} = \frac{EA\sin^3\omega}{h_c^2}$$

$$G_{\text{tet}} = \frac{EA\sin^3\omega}{\sqrt{3}h_c^2} \tag{A.3}$$

$$G_{\text{Kagome}} = \frac{6\sqrt{2}EA\cos^2\omega}{4\sqrt{3}h_d^2}$$

For the pyramid, tetrahedral, and Kagome configurations, ω are 45°, 55.7°, and 55.7°, respectively. According to Eq. (14), the shear stiffness of the sandwich panel with pyramid configuration cores can be expressed as

$$\begin{aligned}
C_{\text{pyramid}} &= G_{\text{pyramid}}h_c = \frac{h_c\bar{\rho}E}{2}\sin^4\omega = \frac{1}{8}\bar{\rho}Eh_c \\
C_{\text{tet}} &= G_{\text{tet}}h_c = \frac{\sqrt{2}\bar{\rho}Eh_c^2}{4\sqrt{3}}\sin^3\omega = \frac{1}{9}\bar{\rho}Eh_c \\
C_{\text{Kagome}} &= G_{\text{Kagome}}h_c = \frac{\rho E\cos^2\omega}{3} = \frac{1}{9}\bar{\rho}Eh_{\text{c}}
\end{aligned} \tag{A.4}$$

NOMENCLATURE

A_{mn}	=	Fourier constant coefficients
a	=	Sandwich panel length
B_{mn}	=	Fourier constant coefficients
C	=	Shear stiffness of sandwich panels
C_{mn}	=	Fourier constant coefficients
D	=	Flexural rigidity of sandwich panels
E	=	Modulus of the material
G_{c}	=	Equivalent shear modulus of the lattice truss core
h_{c}	=	Core thickness
h_{p}	=	Sandwich panel thickness
K	=	Matrix of constant coefficients related to geometry
K_G	=	Matrix of constant coefficients related to thermal effects
m	=	Number of expansion
M_x	=	Bending moment in x-direction
M_{xy}	=	Torsional moment
M_y	=	Bending moment in y-direction
n	=	Number of expansion
N_x, N_y, N_{xy}	=	Compressive in-plane force
Q_x, Q_y	=	Shear force
t	=	Thin plate thickness
u	=	Displacement in x-direction
$[u]$	=	Matrix of Fourier constant coefficients
v	=	Displacement in y-direction
w	=	Displacement in z-direction
w_0	=	Displacement at the middle-plane
K_G	=	Matrix of constant coefficients related to thermal effects
α	=	Coefficient of thermal expansion of the sandwich panel

ΔT_{cr}	=	Critical temperature
μ	=	Poisson's ratio
ϕ_x, ϕ_y	=	Rotations of the normal in the *xz* and *yz* planes

FUNDING

Financial support from the National Natural Science Foundation of China (Grant Nos. 91016025, 11332011, 91216303, and 11472276) and Funds of Science and Technology granted to the Scramjet Laboratory are gratefully acknowledged.

REFERENCES

1. V. Deshpande, M. Ashby, and N. Fleck, Foam Topology: Bending Versus Stretching Dominated Architectures, *Acta Materialia*, vol. 49, pp. 1035–1040, 2001.
2. V. Deshpande, N. Fleck, and M. Ashby, Effective Properties of the Octet-Truss Lattice Material, *Journal of the Mechanics and Physics of Solids*, vol. 49, pp. 1747–1769, 2001.
3. A. G. Evans, J. W. Hutchinson, and M. F. Ashby, Multifunctionality of Cellular Metal Systems, *Progress in Materials Science*, vol. 43, pp. 171–221, 1998.
4. L. J. Gibson and M. F. Ashby, *Cellular Solids: Structures and Properties*, Cambridge University Press, New York, 1997.
5. Q. H. Qin and T. J. Wang, An Analytical Solution for the Large Deflections of a Slender Sandwich Beam with a Metallic Foam Core under Transverse Loading by a Flat Punch, *Composite Structures.,* vol. 88, pp. 509–518, 2009.
6. H.-W. Song, Q.-J. He, J.-J. Xie, and A. Tobota, Fracture Mechanisms and Size Effects of Brittle Metallic Foams: In Situ Compression Tests Inside SEM, *Composites Science and Technology*, vol. 68, pp. 2441–2450, 2008.
7. J. C. Wallach and L. J. Gibson, Mechanical Behavior of a Three-Dimensional Truss Material, *International Journal of Solids and Structures*, vol. 38, pp. 7181–7196, 2001.
8. T. J. Lu, Heat Transfer Efficiency of Metal Honeycombs, *International Journal of Heat and Mass Transfer*, vol. 42, pp. 2031–2040, 1998.
9. Q. H. Qin and T. J. Wang, Low-Velocity Heavy-Mass Impact Response of Slender Metal Foam Core Sandwich Beam, *Composite Structures*, vol. 93, pp. 1526–1537, 2011.
10. J. F. Rakow and A. M. Waas, Thermal Buckling of Metal Foam Sandwich Panels for Convective Thermal Protection Systems, *Journal of Spacecraft and Rockets*, vol. 42, pp. 832–844, 2005.
11. J. F. Rakow and A. M. Waas, Response of Actively Cooled Metal Foam Sandwich Panels Exposed to Thermal Loading, *AIAA Journal*, vol. 45, pp. 329–336, 2007.
12. K. I. Salas and A. M. Waas, Convective Heat Transfer in Open Cell Metal Foams, *Journal of Heat Transfer-Transactions of the ASME*, vol. 129, pp. 1217–1229, 2007.
13. H.-W. Song, Z.-J. Fan, G. Yu, Q.-C. Wang, and A. Tobota, Partition Energy Absorption of Axially Crushed Aluminum Foam-Filled Hat Sections, *International Journal of Solids and Structures*, vol. 42, pp. 2575–2600, 2005.
14. B. Wang and G. D. Cheng, Design of Cellular Structures for Optimum Efficiency of Heat Dissipation, *Structural and Multidisciplinary Optimization*, vol. 30, pp. 447–458, 2005.
15. M. Ashby and Y. Brechet, Designing Hybrid Materials, *Acta Materialia*, vol. 51, pp. 5801–5821, 2003.
16. V. S. Deshpande and N. A. Fleck, Collapse of Truss Core Sandwich Beams in 3-point Bending, *International Journal of Solids and Structures*, vol. 38, pp. 6275–6305, 2001.

17. A. Evans, J. Hutchinson, N. Fleck, M. Ashby, and H. Wadley, The Topological Design of Multifunctional Cellular Metals, *Progress in Materials Science*, vol. 46, pp. 309–327, 2001.
18. G. W. Kooistra, V. S. Deshpande, and H. N. Wadley, Compressive Behavior of Age Hardenable Tetrahedral Lattice Truss Structures Made from Aluminium, *Acta Materialia.*, vol. 52, pp. 4229–4237, 2004.
19. H. N. Wadley, N. A. Fleck, and A. G. Evans, Fabrication and Structural Performance of Periodic Cellular Metal Sandwich Structures, *Composites Science and Technology*, vol. 63, pp. 2331–2343, 2003.
20. E. A. Thornton, Thermal Structures—Four Decades of Progress, *Journal of Aircraft*, vol. 29, pp. 485–498, 1992.
21. A. Mossavarali and M. R. Eslami, Thermoelastic Buckling of Plates with Imperfections Based on a Higher Order Displacement Field, *Journal of Thermal Stresses*, vol. 25, pp. 745–771, 2002.
22. B. L. Fu, *Energy Principle of Elasticity and its Application*, Science Press, China, 2004.
23. K. K. Raju, N. R. Naidu, and G. V. Rao, Thermal Buckling of Circular Plates with Localized Axisymmetric Damages, *Computers & Structures*, vol. 60, pp. 1105–1109, 1996.
24. E. Reissner, On Small Bending and Stretching of Sandwich-Type Shells, *International Journal of Solids and Structures*, vol. 13, pp. 1293–1300, 1997.
25. N. J. Hoff, *Bending and Buckling of Rectangular Sandwich Panels*, NACA TN 2225, National Advisory Committee for Aeronautics, USA, 1950.
26. Q.-H. Tu, General Equations of Sandwich Plates under Transverse Loads and Edgewise Shears and Compressions, *Acta Physica Sinica*, vol. 10, pp. 395–412, 1954.
27. A. V. Lopatina and E. V. Morozovb, Buckling of a Uniformly Compressed Composite Rectangular CCCC Sandwich Plate, *Composite Structures*, vol. 108, pp. 332–340, 2014.
28. J. Chen, W. Liu, and X. Su, Vibration and Buckling of Truss Core Sandwich Plates on an Elastic Foundation Subjected to Biaxial In-plane Loads, *Computers Materials and Continua*, vol. 24, pp. 163–182, 2011.
29. A. M. Al-Khaleefi and H. R. H. Kabir, On the Thermal Buckling Response of Shear-Flexible All-Edge Clamped Rectangular Plates, *Journal of Vibration and Control*, vol. 9, pp. 495–506, 2003.
30. H. Kabir and R. Chaudhuri, Free Vibration of Clamped, Moderately Thick, Arbitrarily Laminated Plates Using a Generalized Navier's Approach, *Journal of Sound and Vibration*, vol. 171, pp. 397–410, 1994.
31. H. J. Rathbun, F. W. Zok, and A. G. Evans, Strength Optimization of Metallic Sandwich Panels Subject to Bending, *International Journal of Solids and Structures*, vol. 42, pp. 6643–6661, 2005.